Especially Significant New Component of N_2O Quantum Yield in the UV Photolysis of O_3 in Air

Sheo S. Prasad

Creative Research Enterprises, 6354 Camino del Lago, Pleasanton, California 94566

Received: April 7, 2005

This paper presents an alternate three-component model for the density ([M]) and temperature (T) dependence of the N_2O quantum yields (ϕ_{N_2O}), in the UV photolysis of O_3 in air, from Estupiñán et al.'s (ENLCW's) high-quality experiments that were a breakthrough in the pressure and T coverage. The three components consist of a new [M]-independent component, the ENLCW-discovered $[M]^1$ component, and the $[M]^2$-dependent component found by Kajimoto and Cvetanovic. The $[M]^1$ component is T independent. The weak T dependence of ENLCW's ϕ_{N_2O} results from the T dependence of the other two components. The agreement of the three-component model with the observed ϕ_{N_2O} is much better than that of ENLCW's one-component (T-dependent linear-in-[M]) model. For example, the percentage residual for a significant two-thirds of all data is better than ±8% in the three-component model compared to only one-third for the ENLCW model. The improvements due to the three-component model are real in the sense that they are obvious despite the experimental error bars in that pressure−temperature domain where the reality is expected to reveal itself in the ENLCW experiment. Also, the new [M]-independent component is nonzero positive at a very high confidence level of 97.5%, sharply contrasting with the current perception. The [M]-independent component is especially significant despite being small compared to the dominant $[M]^1$ component. It implies N_2O formation from excited O_3, tentatively $O_3(^3B_1)$, immune from ENLCW and Prasad controversy over the origin of the $[M]^1$ component. In the suggested interpretation, the $[M]^0$ component varies linearly with $[O_3]$ in the photolyzed O_3/air mixture. Further experiments with $[O_3]$ fixed at various amounts, while the air density and temperature are varied, could check the interpretation. Further computational-chemistry studies to better characterize the low-lying triplet states of O_3 would also help.

1. Introduction

Understanding how simple gas phase reactions occur on excited electronic state surfaces is one of the major challenges facing the fields of reaction dynamics and kinetics. The formation of nitrous oxide (N_2O) in the photolysis of $O_3/O_2/N_2$ mixtures is one of the useful test beds for the investigation of excited state chemical kinetics because N_2 and O (^3P) do not lead to bound N_2O, the exothermic reaction $O_3(X\ ^1A_1) + N_2 \rightarrow N_2O + O_2$ is spin forbidden, and the reaction $N_2 + O_2(X\ ^3\Sigma) \rightarrow N_2O + O$ is highly endothermic. Additionally, N_2O is a climatically important greenhouse gas as well as the dominant source of NO (via the reaction $N_2O + O(^1D) \rightarrow NO + NO$) that catalytically destroys stratospheric O_3. For the past 40 years, therefore, understanding the N_2O quantum yield (ϕ_{N_2O}) in the UV photolysis of $O_3/O_2/N_2$ mixtures has attracted considerable attention.[1]

Kajimoto and Cvetanovic[2] (KC) experiments at high pressures (p) (27 atm ≤ p ≤ 110 atm) established that the ϕ_{N_2O} value due to the three-body $O(^1D)$, N_2 association ($O(^1D) + N_2 + M \rightarrow N_2O + M$) had a quadratic dependence on pressure (p^2, or equivalently $[M]^2$, at constant temperature (T)), since the nascent highly energized $(N_2...O)^{\#\ \#}$ complex needed multiple collisions for stabilization. Most recently, Estupiñán et al.[3] (ENLCW) reached a significant milestone in laboratory studies of ϕ_{N_2O}. For the first time, they measured ϕ_{N_2O} in the UV (266 nm) photolysis of $O_3/O_2/N_2$ mixtures at various low pressures (extending down to about 200 Torr) and at five different temperatures around room temperature. They also made the remarkable discovery that the quantum yield at the low pressure varied linearly with pressure at constant T. Prasad[4] proposed that reaction R1 dominates over the concurrently occurring $[M]^2$-dependent $O(^1D)$, N_2 association in the production of N_2O at low pressures and gives rise to the observed linear pressure dependence of ϕ_{N_2O}.

$$O_3(^1B_2) + N_2 \rightarrow N_2O^{\#} + O_2{}^{*\#} \qquad \text{(R1)}$$

The symbols # and ∗ in reaction R1 denote, respectively, possible vibrational and electronic excitations. Reaction R1 would occur in the ENLCW experiment, since the $O_3(^1B_2)$ state, which is generally thought to be the state responsible for the Hartley band of O_3 (238 nm ≤ λ ≤ 270 nm), would be created by the absorption of the 266 nm radiation, although some ab initio theoretical calculations place the energy of that state above the energy of 266 nm radiation. There would be a nonzero steady state population of $O_3(^1B_2)$ albeit extremely small due to the 10−20 fs lifetime of $O_3(^1B_2)$ against dissociation. Since at present we do not understand (at the atomic process level) how so very rapidly dissociating species can drive a chemical reaction, it is noteworthy that the DeMore and Raper[5] experiment suggests that short-lived $O_3(2^1A_1)$ also produces N_2O.[4] If this source is upheld by further gas phase experiments, then, as discussed in ref 4, there will be non-negligible atmospheric production of N_2O compared to the negligible production via the ENLCW mechanism (or even the KC mechanism) involving $O(^1D)$.

* E-mail: ssp@CreativeResearch.org.

10.1021/jp058114q CCC: $30.25
Published on Web 09/21/2005

The just mentioned work of this author (ref 4) had concentrated on the component of ϕ_{N_2O} that varies linearly with p (or [M]) at constant T. The question of a possible p-independent component at constant T was not explored. The present paper takes up this unfinished work and to this end further analyzes ENLCW's data. It is now shown that the data support a three-component model of ϕ_{N_2O} consisting of a [M]-independent ($[M]^0$) component and components linear and quadratic in [M] ($[M]^1$ and $[M]^2$). It is also shown that the data support this three-component model much better than they support the one-component (T-dependent linear-in-[M]) ENLCW model. The new $[M]^0$ component suggests N_2O formation from excited O_3, unaffected by the current difference of opinion (ENLCW versus Prasad) about the origin of the $[M]^1$ component. The potential reaction of $O_3(^3B_1)$ with N_2 is tentatively suggested as a physical mechanism for this $[M]^0$ component. Although the ENLCW data has been sufficient for showing the existence and importance of the $[M]^0$ component, more experiments are needed to verify the proposed mechanism. The specifics of needed experiments are discussed. It is hoped that the discussions of this paper will stimulate further experimental and theoretical studies.

2. ENLCW's Experimental Data and Data Interpretation

The experimental data used here are the high-quality ϕ_{N_2O} values observed by ENLCW in the UV (266 nm) photolysis of $O_3/O_2/N_2$. These were obtained using modern laser flash photolysis and nonintrusive N_2O detection via tunable diode laser absorption spectroscopy. ϕ_{N_2O} was measured at 200 Torr $\leq p \leq$ 800 Torr and at five different temperatures. A set of 25 ϕ_{N_2O} values at 25 p and T combinations was measured. Edgar Estupiñán provided these data. ENLCW had noted that their plots of ϕ_{N_2O} versus p at constant T showed intercepts (or p-independent components) that varied systematically with T. The actual values of the intercepts were[6] $(1.25 \pm 1.28) \times 10^{-7}$, $(0.76 \pm 1.88) \times 10^{-7}$, $-(1.25 \pm 2.1) \times 10^{-7}$, $-(1.57 \pm 2.4) \times 10^{-7}$, and $-(1.65 \pm 3.1) \times 10^{-7}$ at 324, 295, 270, 243, and 220 K, respectively. The $\pm$ error bars are at 2σ, where σ is the standard error (StdErr) from the regression analysis. The error bars exceeded the magnitude of the intercept that was nonphysical (negative) below 295 K. ENLCW therefore dismissed the intercept (or the $[M]^0$ component). They also discarded the $[M]^2$ component of ϕ_{N_2O} previously established by KC and proposed a one-component model of ϕ_{N_2O} in the UV photolysis of O_3/air mixtures given by eq 1 below.

$$\phi_{N_2O} = \mathcal{A}(300/T)^{\kappa}[M]\left(\frac{1.0}{1.94 \times 10^{-11}\exp(130/T) + 3.3 \times 10^{-11}\exp(70/T)(22/78)}\right) \quad (1)$$

where $[M] \approx [N_2] + [O_2]$, T = temperature, and $(22/78) = [O_2]/[N_2]$. Equation 1 follows from ENLCW's eq IV for ϕ_{N_2O} and the rate constants adopted by them for the deactivations of $O(^1D)$ by N_2 and O_2. Their analysis of the observed ϕ_{N_2O} yielded $\mathcal{A} = (2.8 \pm 0.1) \times 10^{-36}$, $\kappa = (0.88 \pm 0.36)$.

3. Aspects of the ENLCW Model That Suggest the Need for Further Analysis

The one-component ENLCW model is fundamentally incomplete, and there remains an intriguing possibility that the negative intercepts with a large StdErr changing to positive intercepts at 324 K may have been warning signals of the problems caused by the incompleteness. Specifically, the value $\kappa = 0.88 \pm 0.36$ is grossly inconsistent with the κ value derived from an approach that is less error prone and more straightforward. ENLCW had analyzed their data in multiple steps. First, they examined the data segmented into five sets at the five different temperatures T = 324, 295, 243, 270, and 220 K. Three of these sets had only four data points that are rather small. The $\partial\phi/\partial p$ values at the five temperatures were then analyzed to determine the $\kappa = 0.88 \pm 0.36$ value of eq 1.

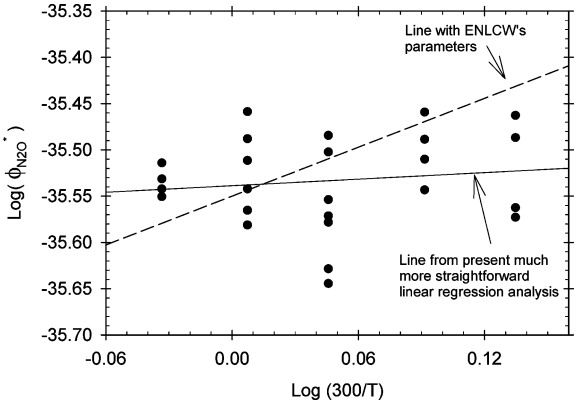

Figure 1. Plot of the logarithm of ϕ_{N_2O}* against log(300/T). If the one-component ENLCW model is a good model for the [M] and T dependence of ϕ_{N_2O}, then the data points should have closely clustered along the straight line marked "line with ENLCW's parameters", but they do not. Furthermore, the problem of data not clustering closely along the linear regression line persists for the line from the present much more straightforward, single-step, linear regression analysis. These cast doubt on the adequacy of the one-component T-dependent linear-in-[M] model. Also, the vast difference in the two regression lines highlights the risk of sole reliance on the results of multistep regression.

The ENLCW approach is both desirable and essential for determining the broad features of the data (such as the first-order dependence on p or [M]). However, in multistep analysis, there is a serious risk that buildup of errors at each step and substep could result in a misleading model. It is therefore most urgent to check the results either through an alternate, single-step regression analysis of all of the data (if possible) or through an examination of various other aspects of the model (such as the presence of undesirable trends, size of the residuals, that is, the differences between the measured and modeled ϕ_{N_2O}). The desirability of constructing a better model becomes evident when these checks are applied.

The first check is quite easily applied, and all of the data (25 p or [M], T, and ϕ_{N_2O} combinations) can be easily analyzed as one set in a single step with the ENLCW model. This is obvious by transforming eq 1 into eq 1*, which is linear rather than nonlinear and allows a look at all of the data in just one plot of log(ϕ_{N_2O}*) versus log(330/T).

$$\log \phi_{N_2O}^* = \log \mathcal{A} + \kappa \log(300/T) \quad (1^*)$$

In eq 1*, $\phi_{N_2O}^* = \phi_{N_2O}(1.94 \times 10^{-11}\exp(130/T) + 3.3 \times 10^{-11}\exp(70/T)(22/78)/[M]$. Figure 1 shows the plot of log ϕ_{N_2O}* versus log(300/T). Had the ENLCW model been a good model for the their data, the data points should have closely clustered around the dashed line in the figure that has a slope of 0.88 and an intercept of -35.55 and is marked "line with ENLCW's parameters". This is not found. Rather than clustering around that line, the data points show quite a scatter. A linear regression of log ϕ_{N_2O}* with log(300/T), shown by the solid line, has a slope of 0.117 with a large StdErr of 0.184 (that exceeds the parameter value). The gross inconsistency between the present

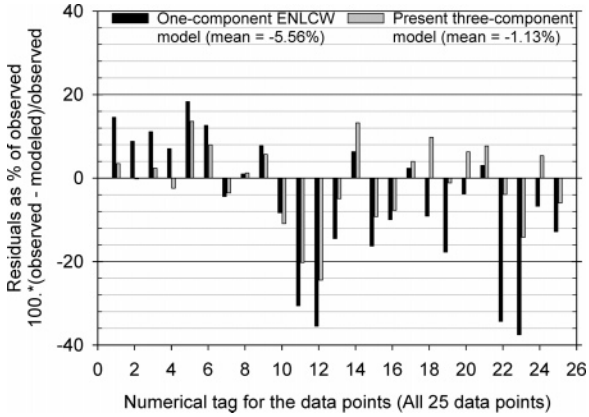

Figure 2. Bar plot (in solid, dark color) of the % residuals for ENLCW's one-component model. The data points are tagged by a serial number. Numbers 1−4, 5−10, 11−17, 18−21, and 22−25 correspond to the data at 324, 295, 270, 243, and 220 K, respectively. For the bars belonging to a given *T*, *p* or [M] increases with increasing serial number. For a good model, residuals should not exhibit any clear trend. In contrast, the solid, dark bars show that the one-component ENLCW model underestimates the observations at 324 K and begins to overestimate them as *T* decreases toward 220 K. The gray-shaded bars are for the % residuals corresponding to the present three-component model (discussed in section 5). It is intended to provide an objective and highly sensitive side-by-side comparison of the ENLCW model and the present model for the entire 25 data points in one glance, compared to only visual inspection of the side-by-side plots of the observed and modeled ϕ_{N_2O}. It is seen that the gray-shaded bars do not show systematic underestimation at $T = 324$ K and overestimation at lower *T*.

κ and ENLCW's κ and the associated StdErr corroborates the suspicion of error built in ENLCW's multistep analysis. More importantly, the problem of observational data not clustering along the regression line is seen with the present linear regression line also. This casts doubt on the adequacy of the one-component *T*-dependent linear-in-[M] model and calls for attempts to build a model that may be in better agreement with the data.

Even if one chooses to disregard this doubt, there is the undesirable trend that is best appreciated from the bar plot of percentage residuals (% residuals) shown in Figure 2 by solid, dark colored bars. The data points in this figure are tagged by a serial number. Numbers 1−4, 5−10, 11−17, 18−21, and 22−25 correspond to the data at 324, 295, 270, 243, and 220 K, respectively. For the bars belonging to a given *T*, *p* or [M] increases with increasing serial number. The percentage residual (% residual) is defined as the difference between the observed value and the modeled value expressed as the percentage of the observed value and is a very sensitive and objective indicator of how well the model reproduces the observations. The ENLCW model (represented by solid, dark bars) underestimates ϕ_{N_2O} at higher *T* (or data points 1−4 belonging to $T = 324$ K). As *T* decreases, the underestimation systematically turns into an overestimation for the data points numbered 11−25 belonging to $T \leq 295$ K. This again calls for an effort to improve the ENLCW model so that there is no such bias.

4. Neither the Quantity nor the Quality of Data Are an Issue

The quantity of data is not an issue, since 25 data points are much more than sufficient for determining the two unknowns $\mathscr{A}$ and κ. The quality of the data is also not an issue, since in the same figure the % residuals (shown by gray-shaded bars) calculated with a more complete model (discussed in the next section) are in much better agreement with the observational data (as is quantified in the next section). Possible improvements to ENLCW's one-component model are, therefore, most logically in the inclusion of missing components of ϕ_{N_2O}. The model of ϕ_{N_2O} that includes the missing components and is much better supported by the data is described next.

5. Three-Component Model That Is Much Better Supported by the Data

5.1. Model Description and Justification for Each Component. The three-component model of ϕ_{N_2O}, called for by the ENLCW measured ϕ_{N_2O}, must include KC's $[M]^2$-dependent $O(^1D)$, N_2 association. In contrast, ENLCW did not include that process in their model. Before proceeding further, it is therefore important to ask the following question: "Why should that process be included?" The following two points are relevant in this context. First, the KC process cannot cease to operate at the pressures used in the ENLCW study, although its contribution to ϕ_{N_2O} may become minor, compared to the contribution of the dominant $[M]^1$-dependent component. The reason is that the fundamental molecular property of the nascent highly energized $(N_2...O)^{\#\,\#}$ complex to require multiple collisions for stabilization, in both O_2-poor and O_2-rich gas, cannot change just because the environmental pressure is low. The observed ϕ_{N_2O} values are 1.62×10^{-6} and 1.88×10^{-6} at 796 and 785 Torr, respectively, and at 295 K. The contributions of the $[M]^2$-dependent process at these *p* and *T* values are 2.73×10^{-7} and 2.68×10^{-7} (if KC's eq 14 and their values of "*a*" and "*b*" are used and allowance is made for the fact that only 78% of the nascent $O(^1D)$ will encounter an N_2 molecule). The corresponding values are 1.60×10^{-7} and 1.57×10^{-7} if eq 4 of Prasad[4] and his values of "*a*" and "*b*" are used. Either way, these contributions are comparable to the observed ϕ_{N_2O} value at 295 K at the level of 8−16%. Contributions of this magnitude are sufficient reasons for including the KC process.

A [M]-independent ($[M]^0$) component that decreases exponentially with decreasing *T* and a component that varies linearly with [M] ($[M]^1$) but is *T* independent are the two other components of the present three-component model. Of the three components, the $[M]^0$ component is new. Equation 2 below describes this three-component model.

$$\phi_{N_2O} = \mathscr{C}\exp(-\alpha/T) + m[M] + \beta[M]^2\left(\frac{295}{T}\right)^{\gamma} \qquad (2)$$

[M] in eq 2 is the total number density of $[M] = [N_2] + [O_2]$. In the region 200 Torr $\leq p \leq$ 800 Torr, $\beta[M]^2$ is an extremely accurate simplification of the form of the $[M]^2$-dependent ϕ_{N_2O} value established by KC (namely, $\phi = (x/(x + a))(x/(x + b))$, with $a = 10\,000$, $b = 60$, and $x = [M]$ all in units of 1 atm). This is also a very desirable simplification because it puts a lesser burden on the nonlinear regression analysis codes. The fact that only 0.78 of nascent $O(^1D)$ from O_3 photodissociation would see a N_2 molecule is absorbed in β. Three-body association processes usually increase with a decrease in temperature. The term $(295/T)^{\gamma}$ accounts for this trend of $[M]^2$-dependent three-body $O(^1D)$, N_2 association per the recommendations of DeMore et al.[7]

The [M]-independent first term of eq 2 and the *T*-independent linear-in-[M] term are suggested, in a rather compelling way, by the subset of low-*p* data points where the contribution of the third term falls below 5% and where the neglect of the third term can be tolerated. A nonlinear regression analysis of these data points using only the first two terms of eq 2 yields a fit characterized by the very low StdErr/(parameter value) ratios (<0.05) for each of the three parameters ($\mathscr{C}$, α, and *m*). The

individual magnitude of the % residual (% residual = 100-(observed ϕ_{N_2O} − modeled ϕ_{N_2O})/observed ϕ_{N_2O}) is also low, being <5% in 5 out of 8 data points (~70% of cases). This indicates an overall good fit. In sharp contrast, efforts to fit the subset of low-p data points by either $\phi_{N_2O} = \eta[M](300/T)^{\xi}$ or $\phi_{N_2O} = \eta[M]\exp(-\xi/T)$ yield unsatisfactory results. The value of ξ in the first case is unreliable due to the StdErr exceeding the parameter estimate. In both cases, the magnitude of the % residual (henceforth |% residual|) is quite high (>10% in 5 out of 8 data points in the first case and >19% in 7 out of 8 in the second case). Thus, a T-dependent linear-in-[M] component contradicts the data.

Figure 2 gives an impression that a [M]-independent term that decreases sharply with a decrease in T added to the ENLCW model may ameliorate the problem of the ENLCW model at the higher T value without worsening the already unsatisfactory situation (overestimation) at the lower $T = 220$ K value. The subset of the low-p data points was therefore modeled with $\phi_{N_2O} = \mathcal{C}\exp(-\alpha/T) + \mathcal{M}[M](300/T)^{\kappa}/(1.94 \times 10^{-11}\exp(130/T) + 3.3 \times 10^{-11}\exp(70/T)(22/78))$. This test further magnified the problem with κ and thereby reinforced the conclusion from modeling experiments with $\phi_{N_2O} = \eta[M](300/T)^{\xi}$ or $\phi_{N_2O} = \eta[M]\exp(-\xi/T)$. These considerations justify the choice of the first two terms of the three-component model (eq 2). Note that T independence of the linear-in-[M] component is suggested by Prasad's[4] interpretation of the physical process responsible for that component. In that interpretation, m of eq 2 equals 0.78-(k_1/k_{diss}), where k_1 is the rate coefficient of reaction 1 and k_{diss} is the dissociative lifetime of the electronically excited O_3 involved in reaction 1. Neither k_1 nor k_{diss} is expected to be T dependent. Note that this physical basis for the $[M]^1$-dependent component differs considerably from that of ENLCW (who attributed this component to N_2, $O(^1D)$ association), and in this paper, it is referred to as the ENLCW−Prasad difference.

5.2. Regression Analysis. The value of $(295/T)^{\gamma}$ changes by only a small amount in the temperature range 220 K ≤ T ≤ 324 K for the likely values of γ (~0.6). Furthermore, averaged over the entire ENLCW $p-T$ range, ϕ_{N_2O} may be relatively insensitive to the third term of eq 2, although that term may not be so for some low-T and high-p combinations. It is therefore difficult to simultaneously determine all five parameters ($\mathcal{C}$, α, m, β, and γ) through nonlinear regression analysis. The regression analyses, using SigmaPlot v8 (SPSS) and Mathematica v6 (Wolfram Research) to cross-check, were therefore done with γ ranging from 0.1 to 1.0 in step of 0.2. For each γ value, the absolute(%residuals) (=mean value of the absolute values of the individual residuals calculated as a percentage of the observed ϕ_{N_2O} value) were determined together with the parameter ($\mathcal{C}$, α, m, and β) values and their StdErr. A plot of absolute(%residuals) with γ suggested $\gamma = 0.6$. The StdErr in each of the four other parameters was small for this γ value. It is noteworthy here that the absolute(%residuals) in the present regression analyses (≈7.5%) are far less (by a factor of ≈2) compared to the absolute(%residuals) (≈13.06%) calculated with the ENLCW model. It is equally noteworthy here that $\gamma = 0.6$ is consistent with the recommendation of NASA's Data Evaluation Panel for collisionally stabilized association reactions.

5.3. Regression Analysis Results and Model Evaluation. Values of the model parameters for $\gamma = 0.6$ were $\mathcal{C} = 5.630 \times 10^{-5}$, $\alpha = 1.899 \times 10^3$, $m = 5.452 \times 10^{-26}$, and $\beta = 4.386 \times 10^{-46}$. The StdErr's associated with these parameter values were 5.494×10^{-6} (CV = 9.76%), 5.216 (CV = 0.275%), 3.79×10^{-27} (CV = 6.95%), and 1.36×10^{-46} (CV = 31%), respectively. CV is the StdErr normalized to the parameter being determined and is usually expressed as a percentage of the parameter value. It is used to gauge how accurately the model describes the various characteristics of the data. Smaller CV means better accuracy. The low CVs associated with $\mathcal{C}$, α, and m suggest that the $[M]^0$ and $[M]^1$ components of the model are significant. Specifically, the [M]-independent term is definitely nonzero positive in the $\pm 2.08\sigma$ range or a confidence level of 97.5% which is in sharp contrast with ENLCW's dismissal of this component. The CV in the $[M]^2$-dependent component is relatively larger. This might be a symptom of problem with observational ϕ_{N_2O} local for those few low-T and high-p values at that T where the contribution of the $[M]^2$ term is largest. Such few problems in data are inescapable in even high-quality experiments. Despite its relatively larger CV, it is satisfying to note that after correction for the presence of O_2 in the ENLCW experiment the β value inferred from KC's original model is extremely close (within a few %) to the β value from the present regression analysis.

The present three-component model of ϕ_{N_2O} is a significantly better model for the [M], T dependence of the observed ϕ_{N_2O} value. This can be appreciated by inspecting the gray-shaded bars in Figure 2 for the % residuals for the three-component present model. Comparing the % residual in this way is an objective and a highly sensitive indicator of model performances throughout the entire spectrum of data, compared to visual evaluation of the performances by laying side by side the plots of ϕ_{N_2O}. For a considerable majority of cases, the data are in decisively better agreement with the present (three-component) model relative to the one-component ENLCW model. For slightly greater than $^1/_3$ of the data points, the % residual is better than ±4% in the present three-component model compared to slightly less than $^1/_{12}$ of data points in the case of the ENLCW model. For a significant majority of 17 out of 25 (or $^2/_3$) data points, the % residual is better than ±8% in the case of the present three-component model, compared to only 8 (or slightly less than $^1/_3$) data points in the case of the ENLCW model. Furthermore, unlike the case with Figure 2 for the ENLCW model, the gray bars of the present model show only a negligible (if any) trend. The %residuals (≡mean value of % residual) for these bars (−1.13%) would decidedly lie very close to the zero compared to the same for the bars corresponding to the ENLCW model (= −5.56%) that would lie almost 5 times farther away.

Figure 3 is a bar plot of the partial percentage contributions of the $[M]^0$-, $[M]^1$-, and $[M]^2$-dependent components to the total ϕ_{N_2O} value from the present three-component model. In each case, the $[M]^1$-dependent component dominates with values in excess of 70%. At $T \geq 295$ K, the contribution of the new [M]-independent component approaches a definitely non-negligible level of 20%. The contribution of the $[M]^2$ component lies generally between 10 and 20%. It slightly exceeds 20% in just three cases where it may approach 25%. In retrospect, the intercepts changing from nonphysical negative to physically significant positive in the ENLCW model and the tendency of that model to overestimate and then underestimate (both as T increased) may have been manifestations of distortions due to fitting the data with a one-component model when the data was calling for a three-component model.

6. Additional Comparisons That Suggest the Necessity of the $[M]^0$ Component

Examining the relative performances of various other conceivable modeling scenarios will now further highlight the

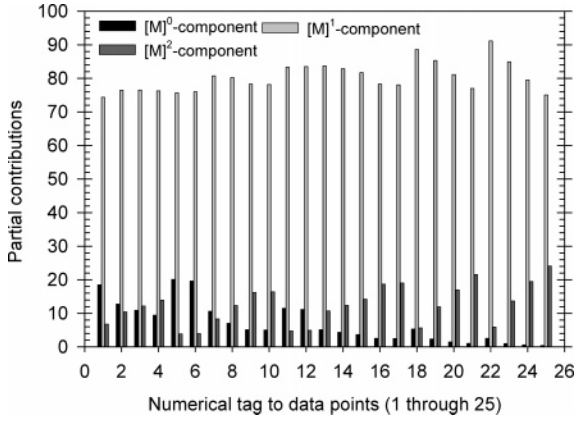

Figure 3. Grouped bar plots of the partial contribution (in percentage of the total) of each of the components of the three-component model. The numerical identification for the groups is the same as that in Figure 2. The leftmost and rightmost bars in any group are respectively the contribution of the [M]-independent and $[M]^2$-dependent components. The middle bar represents the contribution of the *T*-independent linear-in-[M] component. While the linear-in-[M] component dominates, the contributions of the other two are not negligible for those [M], *T* pairs for which those contributions are expected to be important.

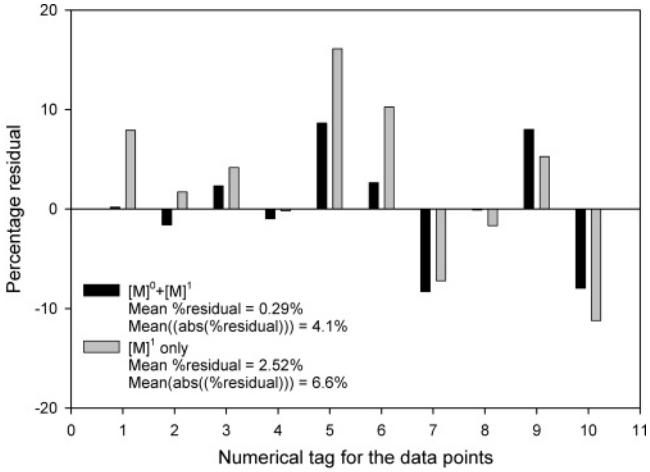

Figure 4. Grouped bar plot of the % residual for the cases of the $[M]^0 + [M]^1$ model (bars with solid, dark color) and the $[M]^1$-only model (bars with gray color) for the set of 10 data points belonging to $T =$ 324 and 295 K. Note the clearly better performance of the $[M]^0 + [M]^1$ model compared with the $[M]^1$-only model.

[M]-independent component and the clearly better performance of the three-component model. Since the *T*-dependent linear-in-[M] model has been shown to be inconsistent with the data (Figure 1 and related discussion), the other modeling options are either the $[M]^1$ (that is, *T* independent), $[M]^0 + [M]^1$, or $[M]^1 + [M]^2$ alternatives to the three-component model. The $[M]^0$ only, the $[M]^2$ only, or their sum are ruled out, since the contributions of $[M]^0$, $[M]^2$, or their sum are minor in the ENLCW pressure regime.

Table 1 shows absolute(%residuals) and %residuals from these comparisons when the models are applied to the entire ENLCW data. Both the absolute(%residuals) and %residuals are decisively larger for the present *T*-independent $[M]^1$ component (9.9 and −3.4%) compared to the same (7.6 and −1.1%) for the more complete three-component model. Inclusion of the $[M]^0$ component results in only marginal change if all 25 data points are considered. One might, therefore, be tempted to conclude that the $[M]^0$ component is insignificant. However, such a conclusion would be wrong. It would be wrong because, in reality, the inclusion of the $[M]^0$ component actually produces remarkable improvements. This point emerges clearly from a closer look at the performances of the $[M]^1$ and the $[M]^0 + [M]^1$ models which reveals that with $[M]^0$ the % residual averaged over 10 data points for $T \geq 295$ K has been remarkably reduced to 1.75% (from 3.4% without the $[M]^0$ component), although the same for 15 data points for $T \leq 270$ K changed from −7.9% (without) to −7.7% (with the $[M]^0$ component). This remarkable improvement (from 3.4% without to 1.75% with) for $T \geq 295$ K is not seen in Table 1, because it is obscured by the expected hardly any change (from −7.9% without to only −7.7% with) for the other 15 out of 25 data points used in constructing Table 1. Thus, the %residuals for all 25 data points remained at −3.9 (=(1.75 × 10 − 7.7 × 15)/25).

The better performance with the inclusion of the $[M]^0$ component comes out even more clearly from a look at the values of absolute(%residuals) and %residuals obtained by fitting the data belonging to $T = 324$ and 295 K only (a set of 10 data points) where the contribution of the $[M]^0$ component is expected to count. These were calculated first with the $[M]^1$ model and then with the $[M]^0 + [M]^1$ model. With the $[M]^0$ component, absolute(%residuals) = 4.1% (versus 6.6% without) and %residuals = 0.29% (versus 2.5% without, i.e., an improvement by an order of magnitude) for these 10 data points. Figure 4 is a bar plot of the residual (in percentages) for each of these 10 data points belonging to 324 and 295 K. In 70% (7 out of 10) data points, the inclusion of the $[M]^0$ component produces a clearly significantly smaller |% residual|. The importance of the $[M]^0$ component can be seen in an alternative way also where we may consider the set of eight data points for which the $[M]^2$ component makes ≤5% contribution. This point was made earlier in paragraph 3 of section 5.1 with respect to an alternate *T*-dependent linear-in-*p* (ENLCW type) model. Here, the comparison is given in the context of the points being made in Table 1. With the $[M]^0$ component, absolute(%residuals) = 9.1% (versus 14.8% without $[M]^0$) and %residuals = −1.8% (versus −4.2% without), confirming the conclusion (about the better performance of the $[M]^0 + [M]^1$

TABLE 1: Comparison of the Various Models Highlighting the $[M]^0$ Component

model	absolute(% residuals)	% residuals	comments
$[M]^1$	9.9	−3.4	incomplete due to omission of the experimentally known $[M]^2$ component; crude in performance relative to the more complete $[M]^0 + [M]^1 + [M]^2$ model
$[M]^0 + [M]^1$	9.6	−3.9	marginal difference with the $[M]^1$-only model deceptively hides the importance of the $[M]^0$ component
$[M]^1 + [M]^2$	leads to unphysical parameters for the $[M]^2$ component as the model struggles to fit higher and lower *T* data *without* the $[M]^0$ component		inconsistent with data; the inconsistency clearly calls for the $[M]^0$ component, since the $[M]^2$ component cannot be neglected
$[M]^0 + [M]^1 + [M]^2$	7.6	−1.1	**best in performance; remains valid over a pressure range exceeding 2 orders of magnitude**

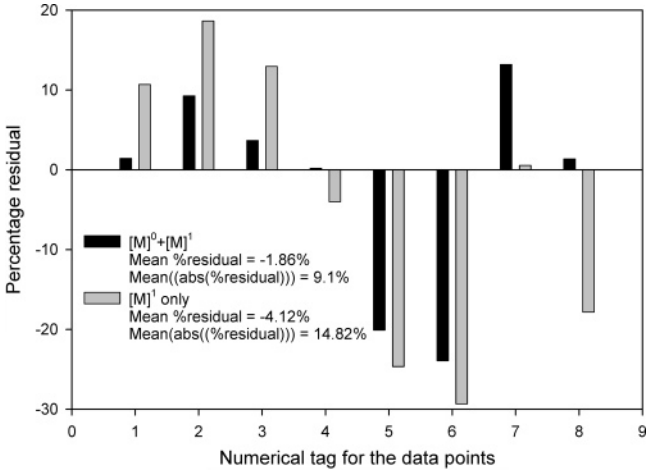

Figure 5. Grouped bar plot of the % residual for the cases of the $[M]^0 + [M]^1$ model (bars with solid, dark color) and the $[M]^1$-only model (bars with gray color) for the set of eight data points for which the contributions of the $[M]^2$ component is ≤5%. Note again the clearly better performance of the $[M]^0 + [M]^1$ model compared with the $[M]^1$-only model.

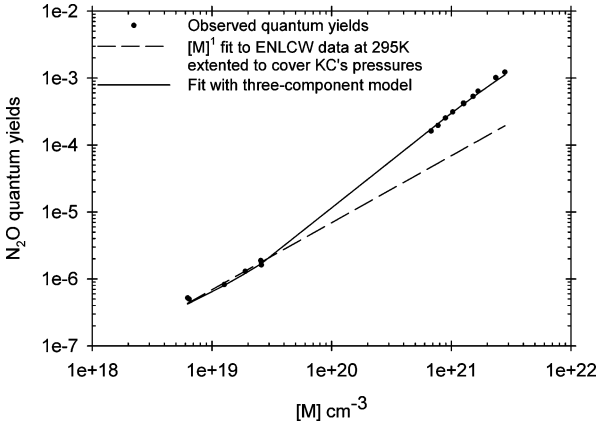

Figure 6. Comparisons of the observed ϕ_{N_2O} values (filled circles) with the two modeled values. The observed ϕ_{N_2O} values are from the ENLCW data at 295 K and KC data also at 295 K (from KC's Table 1). The solid line represents the fit with the present three-component model using the parameters $\mathcal{C}$, α, *m*, and γ from the fit to the ENLCW data and a modification of β as explained in the text (eq 2*). The dashed curve represents the $[M]^1$-only fit with a parameter obtained from fitting the ENLCW data.

model relative to the $[M]^0$-only model) from the consideration of the data at 324 and 295 K. Figure 5 is an analogue of Figure 4. Again, in vast majority (7 out of 8, or ∼90%), the inclusion of the $[M]^0$ component produced a clearly significant reduction in the |% residual|.

The last comparison gives the impression that the $[M]^1 + [M]^2$ model might produce a better result than the $[M]^0 + [M]^1$ model, since in 17 out of 25 data points the $[M]^2$ component contributes more than 5% of the ϕ_{N_2O} value. A test of this possibility gave just the opposite (but highly revealing) result. For this test, the observed ϕ_{N_2O} values were modeled with the two-component $[M]^1 + [M]^2$ model (using the last two terms of eq 2). The modeling was done in two ways: by letting the regression determine *m* and β (keeping $\gamma = 0.6$) and by letting the regression analysis determine *m*, β, and γ of the truncated eq 2. A nonphysical result was obtained in both cases. The standard error in β is unacceptably large in the first case when both *m* and β are determined by nonlinear regression over all 25 data points. This is unacceptable, since β becomes negative in parts of the $\pm 2\sigma$ range. The parameter γ becomes negative in the second case when *m*, β, and γ are determined by the nonlinear regression analysis. This also is unacceptable, since $\gamma < 0$ for collisionally stabilized $O(^1D)$, N_2 association is contradicted by DeMore and Raper (ref 5) experiment. Thus, the $[M]^1 + [M]^2$ model is inconsistent with the observed ϕ_{N_2O} values in the ENLCW pressure regime. The failure of the $[M]^1 + [M]^2$ model, however, does not mean that ENLCW data invalidate the $[M]^2$ component of the ϕ_{N_2O} value in the UV photolysis of O_3 in air that has been so very well established by KC's experiment. Quite the contrary, the failure reinforces the importance of the $[M]^0$ component. The $[M]^1 + [M]^2$ model fails not because the $[M]^2$ is invalid but because the contribution of the $[M]^2$ component in the ENLCW pressure regime is comparable to the contribution the $[M]^0$ component that the $[M]^1 + [M]^2$ model omits. In the absence of the $[M]^0$ term, the $[M]^1 + [M]^2$ model struggles to compensate for the omitted $[M]^0$ component (or the underestimation of ϕ_{N_2O} by $[M]^1$ alone at $T = 324$ and 295 K) by driving γ negative. This assessment is suggested by the fact that the three-component ($[M]^0 + [M]^1 + [M]^2$) model leads to a fit that surpasses in quality the fit produced by either $[M]^0 + [M]^1$ or by $[M]^1$ alone. As a corollary, the $[M]^0$ component is really called for. The $[M]^1$-only model is so incomplete that its performance cannot be improved by piecemeal addition of either the $[M]^0$ or $[M]^2$ component. Both components are need to produce a significant improvement (global reduction of absolute(%residuals) from 9.9 to 7.6% and global reduction of %residuals from −3.4 to just −1.1%). While the need for the $[M]^2$ component is already known from the previous work of KC, the present analysis constitutes an empirical demonstration of the need for the previously unrecognized $[M]^0$ component.

Figure 6 is now presented to reinforce the support for the $[M]^0$ component by putting the above discussions in an even bigger context. By combining the ENLCW data at 295 K and KC's data (from their Table 1), the figure presents the observed ϕ_{N_2O} values (the circles) at room temperature for pressures ranging from 192 Torr to 113 atm, that is, a variation in pressures by a factor of about 450. KC's data from their Table 1 only are used, since the rest of KC's data introduce complication due to the O_2 suppression of ϕ_{N_2O}. The dashed curve represents a fit of the ENLCW data with the $[M]^1$-only model. Clearly, the $[M]^1$-only model is inadequate in the bigger context. In contrast, the solid-line curve representing the present three-component model fits all of the data rather satisfactorily. This curve was constructed from the three-component model using the parameters $\mathcal{C}$, α, *m*, and γ from the fit to only the ENLCW data. However, $\beta[M]^2$ of this model (eq 2) was modified so that the modified equation is now the following eq 2*

$$\phi_{N_2O} = 5.63 \times 10^{-5} \exp(-1899/T) + 6.99 \times 10^{-26}\chi[M] + \left(\frac{2.95}{T}\right)^{0.6}\chi\left(3.86 \times 10^{-26}[M] + \frac{[M]}{[M] + 1.98 \times 10^{24}}\right)\left(\frac{[M]}{[M] + 8.98 \times 10^{20}}\right) \quad (2^*)$$

The modification was necessary to conform to the form of the quantum yield (ϕ_{N_2O} behaving as $\phi = (x/(x + a))(x/(x + b))$) at the high pressures $p \geq 27$ atm (experimentally obtained by KC) and to recognize the possible role of the $O_3 \cdot N_2$ dimer at those *p* values (as discussed by this author in ref 4). $\chi = [N_2]/[M]$ recognizes the difference between χ in the ENLCW and KC

experiments (i.e., not all excited O_3 or $O(^1D)$ see N_2 in the ENLCW experiment). Note that the modified expression converges to $\beta[M]^2$ in the ENLCW regime with the value of β being equal to the value (4.386×10^{-46}) from the fit to the ENLCW data using eq 2. Similarly, the value $6.99 \times 10^{-26}\chi$ equals the value of m ($=5.45 \times 10^{-26}$) of eq 2 derived from the regression analysis of the ENLCW data with eq 2. Thus, excepting the $O_3 \cdot N_2$ related 3.86×10^{-26}, every constant of eq 2* is the same as those obtained by fitting to the ENLCW data with the three-component model represented by eq 2. This contrast between the performances of the two models presented in Figure 6 confirms the paramount importance of the $[M]^2$ component in the big picture, despite ENLCW's neglect of this component. Since it would be incorrect to neglect the $[M]^2$ component and the $[M]^1 + [M]^2$ model leads to unphysical parameters in the ENLCW pressure−temperature regime, the $[M]^0$ component is necessary for a good fit, using *one* (unified) model, of all of the data that span the pressure range ~0.25 atm $\leq p \leq$ 113 atm at 295 K and 192 Torr $\leq p \leq$ 802 Torr at T spread over 220 K $\leq T \leq$ 324 K.

7. Comparisons Considering Error Bars Underscore the Reality of Improvements

The considerably improved agreement of the three-component model (that includes the $[M]^0$ component) with the data relative to the one-component (T-dependent linear-in-p) model as evidenced by Figure 2 is real. To appreciate this point, comparisons must be made with due consideration of the observational error bars. Furthermore, to ensure productive results and to see the reality of the $[M]^0$ component, this comparison must emphasize those data points where the errors are the least and the importance (or contribution) of the $[M]^0$ component is the most. These conditions are satisfied by the data at 324 K. For them, the error bars are ±11.4%. This value follows from the average accuracy of N_2O measurement (= ±16%, taking into account the error introduced by ACUCHEM simulation) and the variation of the intrinsic accuracy of N_2O yield measurement (from ±10.7% at 324 K to ±18.7% at 220 K). These are based on the information presented in ENLCW's paper (their Table 2 and section 3.3.2). The error bars quoted here must be differentiated (as has been done here) from the significantly larger error bars on overall accuracy of the rate constant for N_2, $O(^1D)$ associations reported by ENLCW (i.e., ±27% at room temperature and ±39% at 220 K). This is because the determination of the errors in the rate constants involves considerations of errors in other factors (e.g., that in the determination of the errors in the rate constants for the deactivations of $O(^1D)$ by N_2 and O_2), and those errors are not relevant here. For the data at 220 K, the situation is diametrically opposite to that at 324 K. At 220 K, the error bar is deduced to be ±19.9% (almost a factor of 2 larger) and the effect of the $[M]^0$ component is expected to be the least due to its exponential decrease with decreasing T. Comparisons at these data points will be counterproductive and futile by diluting the importance of the improvements and the importance of the $[M]^0$ component. Both the real improvements at 324 K and its expected dilution at 220 K are seen in Figure 7, which presents a comparison of the observed ϕ_{N_2O} values with the predictions of the one- and three-component models at 324 K (in the top part) and 220 K (in the bottom part).

Figure 7 shows that the predictions of the ENLCW model are either totally outside the observed range dictated by the error bars or are toward the extreme end (both consistently on the underestimation side). In contrast, the predictions of the three-component model are extremely close to observed values without any bias on either the overestimation or the underestimation. At 200 K, the situation is not so decisive. This was, however, expected (due to larger error bars and the lesser importance of the $[M]^0$ component that has been explained earlier) and does not constitute any dilution of the importance of the three-component model.

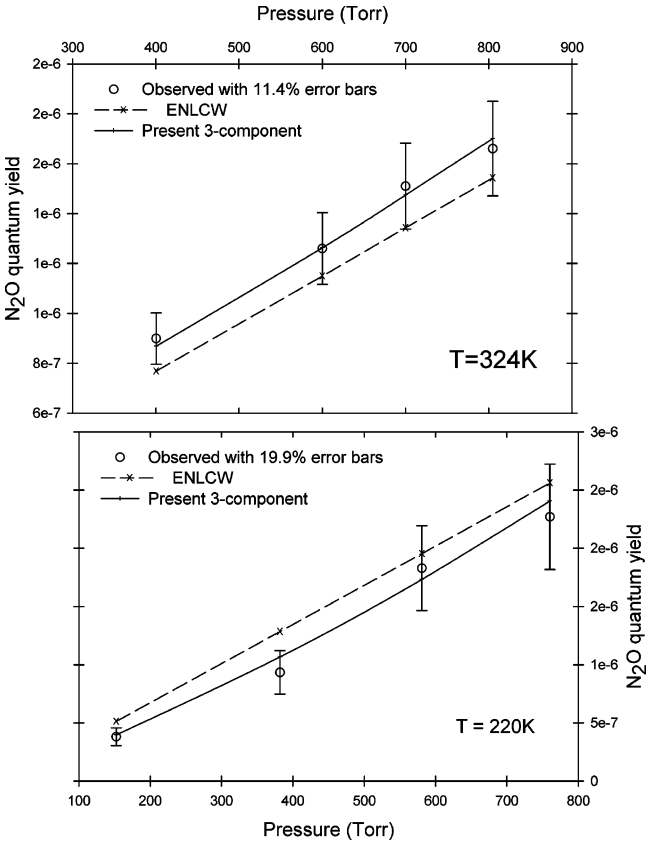

Figure 7. Plots of the N_2O quantum yield against pressure (Torr) for 324 and 220 K with their error bars. The unfilled circles show the observed ϕ_{N_2O} values. The ϕ_{N_2O} values from the one-component ENLCW model are shown by dashed lines and crosses (×). The ϕ_{N_2O} values from the three-component model (eq 2) presented here are shown by solid lines with the + symbol. It shows that the agreement of the present three-component model with the data is considerably better than that with the ENLCW model and that the improved agreement is real, as explained in the text.

8. Special Significance of the [M]-Independent Component for Excited O_3

The [M]-independent component has a special significance, notwithstanding it being minor relative to the dominant $[M]^1$-dependent component when 200 Torr $\leq p \leq$ 800 Torr. It suggests N_2O production from excited O_3, in the gas phase immune from problems such as the differences in ENLCW's and Prasad's theories about the physical processes responsible for the dominant component of ϕ_{N_2O} in the low-pressure regime. Direct $O(^1D)$, N_2 interaction is immediately ruled out, since it would not be [M] independent. Species, other than O_3, that may conceivably be present in the photolysis chamber ($O_2(v)$, $O_2(^1\Delta_g)$, $O_2(^1\Sigma_g)$, translationally hot $O(^3P)$ atoms, etc.) are also readily ruled out. They cannot produce N_2O in ENLCW experiments due to either a significant endothermicity or a high activation energy barrier. For example, $O_2(v)$ even with the highest v possible in the irradiation of O_3 at 266 nm, $O_2(^1\Delta_g)$, and $O_2(^1\Sigma_g)$ produced in the ENLCW experiment do not have the internal energy needed to form N_2O.

8.1. Potential Role of $O_3(^3B_1)$. While ϕ_{N_2O} from the optically pumped singlet O_3 ($O_3(^1B_2)$ and $O_3(2^1A_1)$) has $[M]^1$ dependence, the spin-conserving production of N_2O from collisionally populated, optically forbidden $O_3(^3B_1)$ would be [M] independent for fixed O_3. The relevant properties of the low-lying triplet O_3 are well-known from laboratory[8,9] and theoretical studies.[10]

The O_3*(triplet) would be created in the ENLCW experiment via reaction R2

$$O(^1D) + O_3 \rightarrow O_3^*(\text{triplet}) + O(^3P) \qquad \text{(R2)}$$

which mediates reaction R3.[11]

$$O(^1D) + O_3 \rightarrow O_2 + O + O \qquad \text{(R3)}$$

Low-lying triplet states of O_3 are very short-lived. Most of the rovibrational states of $O_3(^3A_2)$ live much less than 50 ps.[12] The rate coefficient k_2, therefore, controls the rate coefficient k_3. Consequently, $k_2 = 1.2 \times 10^{-10}$ cm^3 molecule^{-1} s^{-1} because $k_3 = 1.2 \times 10^{-10}$ cm^3 molecule^{-1} s^{-1} from DeMore et al.[7] $O_3(^3B_1)$ is the most likely O_3*(triplet) produced in reaction R2, since the electronic energy in $O_3(^3B_1)$ is the best match to the electronic energy in $O(^1D)$ compared to $O_3(^3B_2)$ or $O_3(^3A_2)$.[11]

$O_3(^3B_1)$ is a singly excited state from the in-plane $6a_1$ lone pair orbital to $2b_1\pi^*$ perpendicular to the molecular plane.[10] $O_3(^3B_1)$ and $O_3(^3A_2)$ intersect and have a seam in C_{2v} constrained symmetry.[10] "The seam is crossing in the Franck−Condon region and also near the minimum region of the $^3A_2$ which becomes a conical intersection in C_s symmetry, where these states become the lowest two $^3A''$ states. The lower state is dissociative; it has a saddle point (where it is $^3A_2$) and displacement from the saddle point leads to the ground electronic state products $O_2(^3\Sigma) + O(^3P)$. The upper state, the cone state, is bound ($^3B_1$ at its minimum) and can support vibrational levels."[10] Letting η denote the probability that $O_3(^3B_1)$ from reaction R2 is at its minimum from where it can react, ϕ_{N_2O} from reaction R4 is given by eq 3.

$$O_3(^3B_1) + N_2 \rightarrow N_2O + O_2 \qquad \text{(R4)}$$

$$\phi_{N_2O}(O_3(^3B_1)) = \frac{k_2[O_3]\eta}{k_{O1D,N2} + k_{O1D,O2}[O_2]/[N_2]}\left(\frac{k_4}{\tau^{-1}}\right) \qquad (3)$$

In eq 3, $k_{O1D,N2}$ and $k_{O1D,O2}$ are the rate coefficients for the quenching of $O(^1D)$ respectively by N_2 and O_2. τ is the lifetime of $O_3(^3B_1)$ against dissociation via crossing over to $O_3(^3A_2)$.

$\phi_{N_2O}(O_3(^3B_1))$ of eq 3 is [M] independent, since $[O_3]$ was held constant while the air pressure (or [M]) was varied. For a "sanity" check of ϕ_{N_2O} from $O_3(^3B_1)$, eq 3 is approximated as

$$\phi_{N_2O}(O_3(^3B_1)) \sim 5.97 \times 10^{16}\eta k_4\tau \exp(-130/T) = 5.63 \times 10^{-5}\exp(-1899/T) \qquad (4)$$

ignoring (for simplicity of the algebraic equations) the minor quenching of $O(^1D)$ by O_2, using the already stated k_2 and $k_{O1D,N2}$ values from Ravishankara et al.,[13] and approximating $[O_3] = 9.65 \times 10^{15}$ cm^{-3} (based on data in ref 3). The third term in eq 4 is the value of an intercept derived in the present study. Thus, $\eta k_4\tau = 9.43 \times 10^{-22}\exp(-3538/RT)$ cm^3 molecule^{-1}. The T dependence of $\eta k_4\tau$ could be due to the T dependence of either η, k_4, or both. η can be T dependent, for example, if in reaction R2 $O_3(X\ ^1A_1$, higher $v)$ favors access to that portion of the $O_3(^3B_1)$ potential energy surface that can support reaction R4. For a plausibility demonstration, however, T-independent $\eta \rightarrow 1$ and $\tau \rightarrow 1$ ps may be assumed. Thus, $k_4 = 9.43 \times 10^{-10}\exp(-3538/RT)$ cm^3 molecule^{-1} s^{-1} or 2.34×10^{-12} cm^3 molecule^{-1} s^{-1} at 295 K, that is, quite plausible. k_4 can be larger if η is smaller. The [M]-independent but T-dependent component of the observed ϕ_{N_2O} value therefore suggests that reactions of $O_3(^3B_1)$ with N_2 may lead to N_2O production. The idea that $O_3(^3B_1)$ could chemically react, despite its short lifetime of a few picoseconds, should not cause much surprise, because the short-lived (due to predissociation) $O_2(B\ ^3\Sigma)$ state has also been found to react with N_2 and lead to the production of NO.[14]

9. Potential Atmospheric Relevance of the $[M]^0$ Component

The possibility of N_2O production from reaction R4, even if it is upheld by further experiments suggested in the next section, will be of little atmospheric chemistry significance, since the optical excitation of $O_3(^3B_1)$ is highly forbidden and there are not enough $O(^1D)$ in the atmosphere to cause any significant excitation via reaction R2. However, if N_2O production from $O_3(^3B_1)$ occurs, then it opens up an intriguing possibility that N_2O can be produced from $O_3(^3A_2)$, and that possibility may be potentially important for atmospheric chemistry,[15] since appreciable absorption by O_3 attributable to the $O_3(^3A_2) \leftarrow O_3(X\ ^1A_1)$ transition has been experimentally observed by various studies. For example, Wachsmuth and Abel[16] found that the integrated band intensity of $O_3(^3A_2)$ (000) $\leftarrow O_3(X\ ^1A_1)$ (000) around 9.552.915 cm^{-1} ($\sim$1.046 μm) is as high as $(4.5 \pm 0.5) \times 10^{-22}$ cm, and the reason for it being high despite the transition being doubly forbidden (and thereby $O_3(^3A_2)$ being highly metastable) has been explained in various studies cited in ref 16. For instance, according to Minaev and Agren,[17] this may be due to the spin−orbit coupling to the $^1A_2$ state.

This situation is very similar to the situation with respect to the atmospheric significance of N_2O production from O_3 optically excited to the electronic state responsible for the Hartley−Huggins bands.[4] Paralleling the situation with electronically excited triplet O_3, the N_2O production from O_3 electronically excited by the absorption of the Hartley band is insignificant compared to the significant potential formation from O_3 excited by the absorption of the Huggins band.[4] These considerations underscore the fact that snapshots for N_2O formation in the irradiation of air/O_3 mixtures at sparsely sampled wavelengths can be misleading. Future experiments, suggested in the next section, should therefore attempt to rather densely sample the entire O_3 absorption in the Huggins band region (as was done by DeMore and Rapaer[5] in the condensed phase) and the region where the triplet O_3 ($O_3(^3A_2)$) absorbs (that has never been attempted).

10. Suggestions for Further Laboratory and Theoretical Studies

Although the high-quality ENLCW data were sufficient for showing the existence of the [M]-independent component with a high 97.5% confidence level, more experiments are needed to better establish its magnitude and to better understand its physical cause or causes. From the interpretation of the pressure-independent component presented here, the magnitude of this component should vary linearly with the amount of O_3 (see eq 3). Thus, further experiments with O_3 fixed at several different values while the air density and temperature are varied are needed to check the role of $O_3(^3B_1)$. The accuracy of the new experiment must also exceed the accuracy of the ENLCW experiment and should preferably be better than $\pm$10%. Because the [M]-independent component is more important at lower [M],

observations at $p < 200$ Torr would also be very useful. Extension to lower p values will most probably require N_2O detection capabilities with a sensitivity greater than that provided by TDLAS. Nitrous oxide detection using a combination of rapid sweep infrared laser absorption spectroscopy and pulsed quantum cascade lasers[18] selected to efficiently scan selected N_2O mid-infrared absorption features might help. This system can reach a detection limit of at least 100 ppt at 25 Torr with a measurement time of a few minutes. However, this system may be beyond the reach of many laboratory facilities. Fortunately, one could take an alternate experimental approach of making sufficient measurement at $T > 295$ K. This approach is feasible, since the [M]-independent component is more important at higher temperatures, just as it is at $p < 200$ Torr. To see the effects of this component, the experiments must be done with a precision of $\pm 11\%$ or better.

In the context of the ENLCW−Prasad difference over the physical mechanism responsible for the $[M]^1$ component, the T dependence of the $O(^1D)$ quantum yield in O_3 photodissociation at 266 nm may have an importance. Although that T dependence is unknown at present, judging from the recent study of Dunlea et al.,[19] it may decrease with decreasing T. It would be useful to verify this expectation, since it is counter to the T dependence of the ENLCW mechanism of N_2O production from $O(^1D)$.

The proposed tentative $O_3(^3B_1)$ mechanism for the [M]-independent component is critically dependent on the assumed properties of $O_3(^3B_1)$ based on the Tsuneda et al. study.[10] Further computational-chemistry studies to better characterize the low-lying triplet states of O_3 would help in either further refining the present proposal or in seeking alternatives. Eventually, experiments with $O_3(^3A_2)$ should also be attempted.

11. Summary

(1) Utilizing the power of nonlinear regression analysis, this paper has reanalyzed the ϕ_{N_2O} values in the UV photolysis of O_3 in air that were carefully measured by Estupiñán et al. (ENLCW) employing some of the best modern laboratory techniques. An alternate model for the [M] and T dependence of the measured yields has been identified from this reanalysis.

(2) The alternate model of ϕ_{N_2O} includes a new hitherto ignored [M]-independent component, the ENLCW-discovered linear-in-[M] component, and the $[M]^2$-dependent component previously found by Kajimoto and Cvetanovic (KC). The $[M]^1$ component of the present model is T independent, and the mild T dependence of ENLCW's ϕ_{N_2O} is due to the T dependence of the other two components.

(3) The support for the three-component model is clearly much better than the support for the T-dependent linear-in-[M], one-component ENLCW model. When the ENLCW model parameters are derived from a more straightforward method using a linear regression on the entire data set of 25 measured ϕ_{N_2O} values in a single step, then one of the two parameters is totally unreliable, suggesting that the model is fundamentally inconsistent with the data. Model incompleteness rather than data deficiencies is indicated as the cause of the inconsistency, because in sharp contrast all of the four parameters of the three-component model that were determined by nonlinear regression analysis showed low standard errors. In particular, the confidence level for the [M]-independent term being nonzero positive is very high (97.5%). The magnitudes of the individual percentage residual and the %residuals are also significantly better in the case of the three-component model than those in the one-component model. For example, for 17 out of 25 (or $^2/_3$) data points the % residual is better than $\pm 8\%$ in the case of the present three-component model, compared to only 8 (or slightly less than $^1/_3$) data points in the case of the ENLCW model. Comparison of the performances of the present model and the ENLCW model, taking into account the observational error bars, shows that the improved performance of the present model is real.

(4) Comparison of the performances of the various models $[M]^0$, $[M]^0 + [M]^1$, $[M]^1 + [M]^2$, and $[M]^0 + [M]^1 + [M]^2$ specifically shows that the present model produces a good fit of all of the data that span the pressure range ~ 0.25 atm $\leq p \leq 113$ atm at 295 K and 192 Torr $\leq p \leq 802$ Torr at T spread over 220 K $\leq T \leq 324$ K.

(5) The new [M]-independent component found here has a special significance. It implies N_2O formation from excited O_3, immune from a problem like the differing ENLCW and Prasad ideas about the origin of the linear component experimentally discovered by ENLCW.

(6) Tentatively, $O_3(^3B_1)$ is proposed as the excited O_3 responsible for the [M]-independent component via the potential reaction $O_3(^3B_1) + N_2 \rightarrow N_2O + O_2$. In this interpretation, the pre-exponential term in the $[M]^0$ component varies linearly with O_3 number density ($[O_3]$) in the photolyzed O_3/air mixture.

(7) Although the ENLCW data have been sufficient for showing the existence and importance of the [M]-independent components, experiments with $[O_3]$ fixed at various amounts, while the air pressure and temperature are varied, are needed to test the proposed interpretation. Further computational-chemistry studies to better characterize the low-lying triplet states of O_3 would also help.

Acknowledgment. The research was supported by the NASA grant NNG04GL29G. Edgar Estupiñán's providing the observational data is gratefully appreciated. Without his admirable willingness to share the data, this investigation could not have taken place. Also appreciated are Paul H. Wine's scientific vision and efforts in getting the ENLCW experiments done. I have learned a lot from these high-quality, record-setting experiments.

References and Notes

(1) DeMore, W. B.; Davidson, N. *J. Am. Chem. Soc.* **1959**, *81*, 5869. Norrish, R. G. W.; Wayne, R. P. *Proc. R. Soc. London, Ser. A* **1965**, *288*, 200.
(2) Kajimoto, O.; Cvetanovic, R. J. *J. Chem. Phys.* **1976**, *64*, 1005.
(3) Estupiñán, E. G.; Nicovich, J. M.; Li, J.; Cunnold, D. M.; Wine, P. H. *J. Phys. Chem. A* **2002**, *106*, 5880.
(4) Prasad, S. S. *J. Chem. Phys.* **2002**, *117*, 10104.
(5) DeMore, W. B.; Raper, O. F. *J. Chem. Phys.* **1962**, *37*, 2048.
(6) Estupiñán, G. Ph.D. Thesis, Georgia Institute of Technology, Atlanta, GA, 2001.
(7) DeMore, W. B.; Golden, D. M.; Hampson, R. F.; Howard, C. J.; Kolb, C. E.; Kurylo, M. J.; Molina, M. J.; Ravishankara, A. R.; Sander, S. P. *Chemical Kinetics and Photochemical Data for Use in Stratospheric Modeling: Evaluation Number 12*; JPL Publication 97-4: 1997.
(8) Garner, M. C.; Hanold, K. A.; Sowa Resat, M.; Continetti, R. E. *J. Phys. Chem. A* **1997**, *101*, 6577.
(9) Anderson, S. M.; Mauersberger, K. *J. Geophys. Res.* **1995**, *100*, 3033.
(10) Tsuneda, T.; Nakano, H.; Hirao, K. *J. Chem. Phys.* **1995**, *103*, 6520.
(11) Amimoto, S. T.; Force, A. P.; Wiesenfeld, J. R. *Chem. Phys. Lett.* **1978**, *60*, 40.
(12) Abel, B.; Charvat, A.; Deppe, S. F. *Chem. Phys. Lett.* **1997**, *277*, 347.
(13) Ravishankara, A. R.; Dunlea, E. J.; Blitz, M. A.; Dillon, T. J.; Heard, D. E.; Pilling, M. J.; Strekowski, R. S.; Nicovich, J. M.; Wine, P. H. *Geophys. Res. Lett.* **2002**, *29*, 1745.
(14) Zipf, E. C.; Prasad, S. S. *Science* **1998**, *297*, 211.
(15) Prasad, S. S. *J. Geophys. Res., [Atmos.]* **1997**, *102*, *21*, 527.
(16) Wachsmuth, U.; Abel, B. *J. Geophys. Res.* **2003**, *108* (D15), 4473.
(17) Minev, B.; Agren, H. *Chem. Phys. Lett.* **1994**, *217*, 531.
(18) Nelson, D. D.; Shorter, J. H.; McManus, J. B.; Zanhiser, M. S. *Appl. Phys.* **2002**, *B75*, 342.
(19) Dunlea, E. J.; Ravishankara, A. R.; Strekowski, R. H.; Nicovich, J. M.; Wine, P. H. *Phys. Chem. Chem. Phys.* **2004**, *6*, 5484.